IEEE Access
Multidisciplinary | Rapid Review | Open Access Journal

Received November 19, 2018, accepted December 10, 2018, date of publication December 25, 2018,
date of current version February 4, 2019.

Digital Object Identifier 10.1109/ACCESS.2018.2889717

Utilizing Active Sensor Nodes in Smart Environments for Optimal Communication Coverage

TAO XIE[1], CHUNJIONG ZHANG[2], ZHENGWAN ZHANG[3], AND KAI YANG[2]
[1]College of Computer and Information Sciences, Southwest University, Chongqing 400715, China
[2]College of Electronics and Information Engineering, Tongji University, Shanghai 201804, China
[3]Online and Continuing Education College, Southwest University, Chongqing 400715, China

Corresponding author: Tao Xie (xietao@swu.edu.cn)

This work was supported in part by the National Natural Science Foundation of China under Grant 61807027, in part by the MOE-China Mobile Research Fund Project under Grant MCM20160405, and in part by the Fundamental Research Fund for the Central Universities of the MOE under Grant SWU118006 and Grant XDJK2012C026.

ABSTRACT Wireless sensor networks are widely used in smart environments to capture and detect the activities of human beings, and achieving reliable transmission between sensor nodes has become one of the main challenges of practical applications. This paper presents a scheme for path planning that is designed to achieve optimal coverage by using active nodes to periodically fill in the blank areas and to replace the failed nodes. This approach can effectively avoid uneven energy consumption while maintaining complete link states. Meanwhile, the curl field of the nodes is used to model the effects of the residual energy and the distance between nodes, thereby effectively relaxing the requirements on the spatial positions of the nodes. Experiments show that in the case of directional transmission, the proposed method demonstrates better performance than other algorithms in terms of the network lifecycle, coverage, and transmission reliability. This method can effectively address the problem of cross-node failure along the transmission paths in complex and dynamic networks.

INDEX TERMS Smart environment, wireless sensor network, reliable transmission, optimal coverage.

I. INTRODUCTION

Pervasive sensing technologies embedded in smart environments have provided unprecedented opportunities for health and safety monitoring. Wireless sensor networks (WSNs) are widely used in smart environments to capture and detect the activities of human beings due to their excellent communication performance and low deployment cost [1], [2]. A WSN contains a large number of sensor nodes that can detect, collect, and process data and then transmit those data to the base station via sink nodes. When hundreds or thousands of sensors are randomly deployed in a WSN, problems regarding shared communication paths and redundancy of the sensor nodes tend to arise [3], which can result in abnormal links or even signal interruption. Since the death of nodes or node hibernation will cause significant changes in the network topology, it is necessary to use the information on the switching of the node states to maintain and update communication routes [4]–[6]. For example, when natural disasters such as landslides or water pollution events occur, information transmission will be interrupted, and gaps in node coverage will form due to the limited wireless communication distance. This problem will be further exacerbated when hundreds of thousands of sensors are randomly deployed. The sensors in such complex environments can be divided into two types. Nodes of the first type are static nodes, which are sensors in fixed positions that are used for passive monitoring tasks; nodes of the second type are active nodes, which are typically mounted on or carried by mobile objects or agents, e.g., moving cars and pedestrians. We use the active node instead of mobile mode to specify that a mobile sensor node have active interaction behavior with the static nodes nearby. That is when these active nodes roam in an area, they will frequently establish and release connections with surrounding static nodes. To ensure that communications between a mobile node and its surrounding static nodes are not interrupted once established, the communication coverage areas of the static nodes must intersect with each other. Therefore, reliable transmission between

sensor nodes has become one of the main challenges faced in deploying WSN-based smart environments.

To find efficient and reliable communication links, control messages broadcast between nodes are typically used [7]. It is assumed that the geographic locations of the sensor nodes can be obtained by GPS receivers. The distances and angles between nodes can also be measured and used to estimate node positions through trilateration, triangulation and maximum likelihood estimation. Examples of indicators that are calculated using this approach include the RSSI (received signal strength indicator), AOA (angle of arrival), TOA (time of arrival) and TDOA (time difference of arrival) [8]. However, this approach is computationally complex and provides limited network accessibility and scalability. To alleviate these problems, it is necessary to establish a communication link that is within the perception range of a node but, at the same time, does not depend on the physical location of the node. Therefore, this paper presents a scheme for path planning that is designed to achieve optimal coverage by using active nodes [9] to periodically fill in blank coverage areas and replace failed nodes. This approach can effectively avoid uneven energy consumption while maintaining complete link states. In addition, the curl field of the nodes is used to model the effects of the residual energy and the distance between nodes, thereby effectively relaxing the requirements on the spatial positions of the nodes.

The remainder of this paper is organized as follows. Section 2 discusses related work. Section 3 presents the proposed method. Section 4 describes the experimental procedure and results, and conclusions are drawn in Section 5.

II. RELATED STUDIES

Currently, the research related to communication through active nodes falls into two main categories: the optimization of network coverage by adjusting node positions and the improvement of the reliability of network transmission by means of mobile nodes.

Data can be collected using either the location-based approach or the multidimensional approach [10]. Location-based data collection can be used to identify the mode of interaction between an active node and other nodes in the environment and enables the analysis of the network topology to find the cause of and solution to a problem. In multidimensional data collection, sensors with different functions are used to collect multifaceted data, including displacement, luminosity, and vibration frequency, in a given monitoring area. The limitation of this approach, however, is that it does not allow the determination of the correct time stamp and energy consumption when the direction of motion changes. To overcome these shortcomings, authors have proposed the use of mobile nodes to effectively solve the problem of reliable transmission in WSNs [11], [12] by replacing static nodes that cover fixed areas with mobile nodes. However, the main disadvantage of this strategy is that the data transmitted by the sink node will be lost when the transmission is incomplete. Since the transmission capacity of neighboring nodes is limited, it is difficult to establish complete communication; in addition, the narrowing of communication coverage will significantly affect the stability of the network topology. Thus, many scholars have proposed different solutions. For example, Dini *et al.* [13] proposed a random motion algorithm (AORDM) for improving network connectivity. Fadlullah *et al.* [14] proposed a dynamic trajectory control algorithm for improving the throughput and delay of a network by adjusting the coordinates of the center nodes and the radius of the coverage area. Additionally, Taifei *et al.* [15] proposed a hierarchical region coverage optimization algorithm based on a genetic algorithm (GACOA) to reduce the network deployment cost and increase the coverage area. However, the complexity of these methods is high, their convergence speeds are limited, and it is still difficult to effectively achieve optimal coverage using sensor nodes. Moreover, Colom *et al.* [16] proposed a routing method called ad hoc on-demand distance vector routing (AODV), in which each mobile node is managed by a dedicated routing protocol. Although this dynamic, self-starting network can repair broken links, this method has serious transmission delay problems.

To achieve optimal coverage, a directional antenna can be used as a wireless base station, and then, circular coverage theory can be used to maximize the total coverage area and time [17]; additionally, the number of static sensors can be increased to improve the quality of network communication while using a first-order grayscale model to obtain the intrusion detection history of the network [2]. This method can be used to effectively determine which communication links are unstable. The downside is that the multipath phenomenon will occur as the node density increases, which will increase the processing load of the sink nodes. In addition, a method based on a confident information communication model has been developed to obtain the optimal configurations of communication links; this method not only considers cooperative communication between processing sensors but also utilizes the relationship between the path length and the hop count in space [18]. Although these methods optimize node coverage, the resulting transmission reliability, robustness, and complexity are not very satisfactory. To address these shortcomings, we propose a novel path planning method. The main contribution of this paper is that it proposes a method of seeking optimal coverage by directing active nodes along the shortest movement path to replace faulty nodes and fill in blank coverage areas.

III. THE PROPOSED METHOD

Depending on the sensor devices, typical network models include disk models, ring models, probabilistic models, fusion-based monitoring models, and directed overlay models. In the disk perception model, the communication radius of a node is closely related to its transmit power [11], [12], [19]. When the distance between nodes exceeds a certain value, an effective communication link cannot be established. We call the maximum distance that can

establish an effective communication link the communicable radius. Obviously, the communication range of a node is a circular area with the node as the center and the communication radius as the radius. Although communication links can be established based on the communicable radius, data transmission may be unstable. For stable transmission, we need a node as a relay to perceive the existence of other nodes. Therefore, we call the maximum distance that can perceive other nodes the perception radius. Similarly, the perception range of a node is a circular area with the node as the center and the perception radius as the radius.

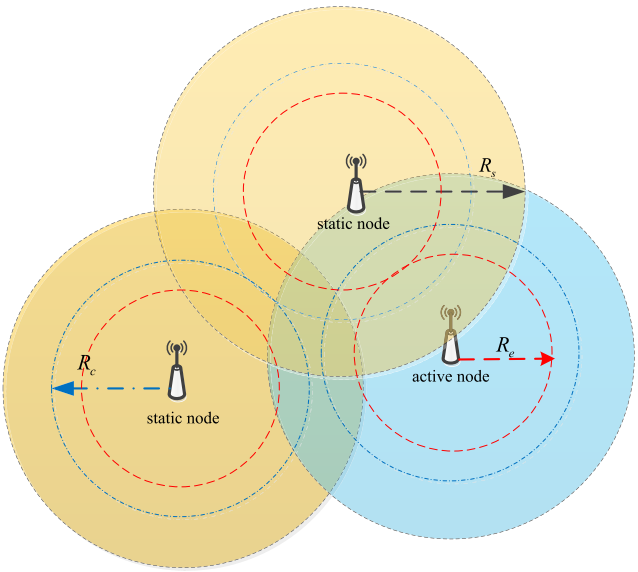

FIGURE 1. A simple network model.

Let R_s, R_c and R_e represent the perception radius, communication radius and coverage radius, respectively, of a node. Then, the perception range, effective communication range and coverage range of the node are circular areas that are centered on the node and have the corresponding radius R. Assume that all nodes have the same communication range and that the communication radius of a node is larger than its coverage radius, as shown in Fig. 1. Under these assumptions, an active node can interact with the static nodes that are within its effective communication range and can determine its own movement trajectory using the coverage information of the static nodes. Given randomly distributed static nodes, the larger the communication radius is, the more unstable the communication quality [2]. When the distance between two nodes is greater than the sum of their effective communication radii, communication will be interrupted. At this time, the active node is required to act as a relay node to establish an effective communication link. This process can be accomplished by means of path planning for the active node.

A. PATH PLANNING FOR ACTIVE NODES

To maximize the coverage area, the repeated displacement of the active nodes should be reduced as much as possible, even if a node moves only a small distance. This requires that the union of the coverage areas of the active nodes and static nodes include the entire monitoring area and that the intersection of them be empty. This is equivalent to finding paths with the smallest encircling rate with respect to motion curves on the movement trajectories of the active nodes such that the paths do not intersect with any covered areas and the line of connected covered areas always intersects with the movement path of each active node. To this end, we use a quadtree to record the location information of the subregions. After the quadtree of the monitoring area has been constructed, the subregions can be traversed through a hierarchical search. When an active node moves to the specified area for mobile coverage, the breadth-first search algorithm is used to scan from the root of the tree until the location of the designated area is identified. Note that the depth of the quadtree affects the efficiency of traversal among regions; this depth value is determined by the monitoring area and the communication capacity of the mobile node.

Theorem 1: After division, the depth of the quadtree is d, $d = \frac{1}{2}\log_2\left(\frac{wh}{2\sin(2\arctan\frac{h}{w})R_c^2}\right)$, where w and h represent the width and height, respectively, of the monitored area.

Proof: Note that the termination condition for the minimum subregion division is that the area of each subregion must be less than or equal to the area of the inscribed rectangle corresponding to the communication range of the active nodes. Let w and h represent the width and height, respectively, of the monitored area; then, the intersection angle θ can be calculated as $\arctan\frac{h}{w}$. Because the subregions are always similar to the whole region regardless of how they are divided, the area of the inscribed rectangle can be calculated as $s = 2\sin(2\arctan\frac{h}{w})R_c^2$. On the other hand, the area of the subregion of depth i is calculated as $s' = \frac{wh}{2^{2i}}$. Because $s' \le s$, we obtain $d = \frac{1}{2}\log_2\left(\frac{wh}{2\sin(2\arctan\frac{h}{w})R_c^2}\right)$.

Using the quadtree structure can enable the effective traversal of all subregions, and the nodes moving between the subregions should avoid the generation of repeated paths. It is easy to prove that if a node traverses the quadtree by means of a breadth-first search, there must be a nonrepeating path that can access each subregion in the area. The goal of movement inside a subregion is to achieve full coverage by moving the least distance.

There are two possible situations:

1) When there is no static node in the subregion, column-row scanning can be used to achieve the optimal coverage of the subregion. The active node initially moves from top to bottom and then moves a distance of $2R_s$ in the horizontal direction after vertical scanning. The active node repeats this process until the whole area has been completely traversed.

2) When there are static nodes in the subregion, as shown in Fig. 2(a), it is necessary to determine whether the area that is not covered by those nodes is connected. If it is connected,

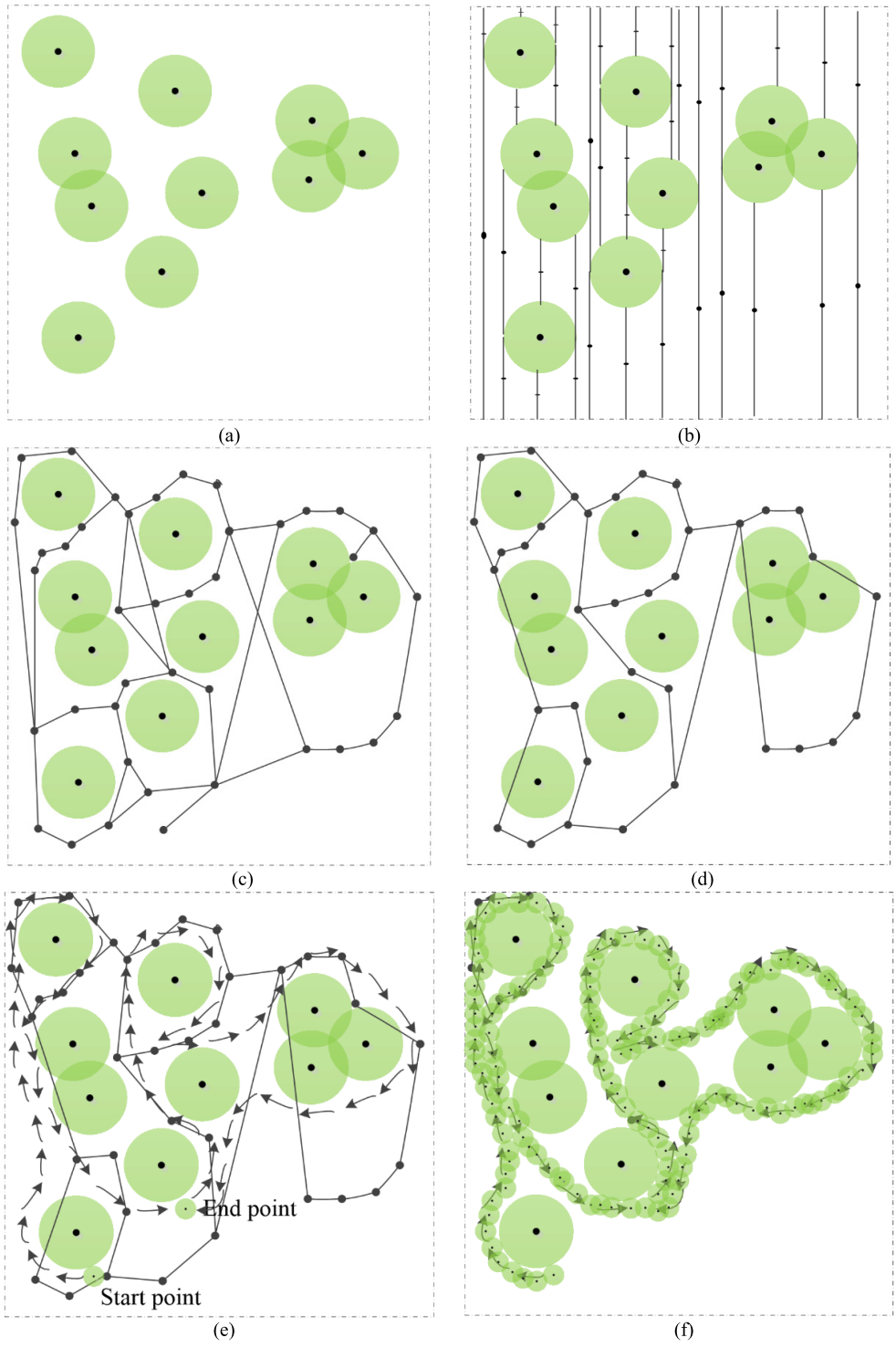

FIGURE 2. Movement in subregions.

the remaining areas can be traversed using column-row scanning; otherwise, we can use the following steps to connect all areas.

Step 1: Find the boundary points of the covered areas and connect those points with straight lines until the boundary of the existing coverage area is reached. Mark the middle point of each line segment, as shown in Fig. 2(b).

Step 2: Find adjacent middle points and connect them sequentially such that the connections do not intersect with the coverage areas, as shown in Fig. 2(c).

Step 3: Modify the movement trajectory such that it becomes an Euler diagram [20], as shown in Fig. 2(d). This is to ensure that the area covered by the movement is connected and disjoint with the area already covered.

Step 4: Optimize the movement trajectory through the following equation:

$$Minimize(\sum_{i=1}^{M} L_i), \quad subject\ to \left(\sum_{i=1}^{M} A_i\right) \bigcup A_{static} \supseteq S$$

where M represents the number of active nodes, A_{static} represents the area covered by the static nodes, A_i is the area covered by node i, $\|A_i\| \leq 2L_iR_s + \pi R_s^2$, and L_i is the movement distance of node i within the monitoring area. L_i can be computed as follows:

$$L_i = \frac{\|s\| - \|A_{static}\| - \pi R_s^2}{2R_s}$$

Step 4 minimizes the sum of the movement distances of all active nodes given the optimal coverage of the network, as shown in Fig. 2(e) and Fig. 2(f). Note that the optimal movement path is affected by many factors, such as the features of the monitoring area and the positions of the nodes. The algorithm needs to avoid the repeated displacement of active nodes during movement and reduce the overlap with the static coverage areas. This problem can be transformed into a traveling salesman problem [21] to yield the approximate optimal solution.

If nodes fail, die or are separated by a large distance in the monitoring area, network coverage gaps can easily occur, preventing the establishment of reliable transmission links. To address this issue, it is necessary to establish a communication field in the network for effectively sensing variations in the node signals. It is known that the Ampère loop theorem has a mechanism for processing induction information, which can be used to characterize self-identification and mutual excitation and enables the use of a constraint on the strength of radio-frequency (RF) signals to form a dynamic equilibrium network [22]. This provides an alternative idea for optimizing the coverage of WSNs, that is, the establishment of a communication field to allow the active nodes to sense the signal strengths of other nodes in the coverage area. In a steady magnetic field, the magnetic induction B is related to the current I in the coil. When $I = 0$, a magnetic field exists nearby, which indicates the presence of a communication-capable node at the edge of the blank coverage area where the active node is located; when the magnetic induction B is zero, there is no current in the space, which suggests that the blank coverage area is large and that multiple active nodes are required to serve as relays to establish a communication link. In this case, a node can use its sensing function to find relay nodes in the communication field, thereby planning its route and determining whether to replace a failed node or fill in a blank coverage area.

B. COMMUNICATION FIELDS IN NETWORKS

The communication field of a node can be represented as a function of the residual energy and node spacing and can be used to obtain the optimal location of the node. In a randomly distributed network, data are transmitted in a multi-hop manner. However, the distance between two static nodes is sometimes relatively large, such that the communication coverage area between the two points is limited, resulting in unstable communication signals. In this case, an active node can be used as an intermediary cascade node to ensure reliable transmission. Assuming that the motion of the node is a function of time, the motion trajectory equation of the active node can be represented [13]–[15] as:

$$\theta(t) = c_0 + c_1 t + c_2 t^2 + c_3 t^3$$

where c_0, c_1, c_2 and c_3 are constant coefficients, and t is the moving time of the active node. According to [11] and [23], the encircling rate of the motion curve of the active nodes can be calculated as:

$$k = \left|\frac{d\theta}{dt}\right| = \frac{\theta''}{(1+\theta'^2)^{3/2}}$$

Because the encircling rate of the movement curve is related to the encircling radius, i.e., $r = \frac{1}{k}$, we can obtain the encircling radius of movement as follows:

$$r = \frac{|2c_2 + 6c_3 t_i|}{(1 + (c_1 + 2c_2 t_i + 3c_3 t_i^2)^2)^{3/2}}$$

Suppose that the distance between two circles is $R_s + l$, where R_s is the radius and l is the disjoint distance between the circles. We use a line segment to connect the centers of the circles and mark the middle points of each segment; then, the active nodes should move along a trajectory passing through these middle points. Since the initial position of the trajectory is on the concentric circle of the outermost region, the distance between the active node and the edge nodes is $R_c/2$. Additionally, because the distance between the edge nodes is $(2R_c + l)/2$, the length of the effective movement path of the active node is calculated as:

$$L = 2\pi \sum_{i=0}^{\frac{R_s+l}{2r}-1} [R_e - (2i+1)r] + 2r\left(\frac{R_s + l}{2r} - 1\right) + \frac{R_c - r}{2}$$

Now, the communication field can be represented in vector form [20], [22]:

$$A(x, y, z) = P(x, y, z)i + Q(x, y, z)j + R(x, y, z)k$$

where x, y and z represent the three-dimensional coordinate axes; i, j and k represent the unit direction vectors; and P, Q and R represent first-order continuous partial derivative functions. Then, the communication range of the edge node of a blank coverage area is a directed surface with a boundary L. According to the Stokes formula [18], we have:

$$\oint A \cdot dS_c = \iint_{S_c} \left(\frac{\partial R}{\partial y} - \frac{\partial Q}{\partial z}\right)dydz + \left(\frac{\partial P}{\partial z} - \frac{\partial R}{\partial x}\right)dzdx + \left(\frac{\partial Q}{\partial x} - \frac{\partial P}{\partial y}\right)dxdy$$

where the expression inside the integral symbol is the curl of the communication path A, denoted by $rotA$. Here, the curl represents the density of the lines in the closed field around the node, which is used to simulate the radius of the RF signal.

This equation represents that the effective communication coverage of a node with communication range S_t traveling on path A along the directed curve L is equal to the value of the curl *rotA*. If the edge node produces a velocity field for communication coverage that is steadily fluid and has no Doppler effect [24], then $\int_L A \cdot dS_c$ represents the total effective communication coverage per unit time, representing the strength of the communication signal of the active node when it moves along L. When $rotA = 0$, the active node cannot communicate while it moves.

The curl can be divided into an internal curl or an external curl depending on whether the active node can perceive the RF signals of static nodes. If the active node can receive signals from static nodes, we call the corresponding line density in the closed field the internal curl; otherwise, we call it the external curl. Obviously, the internal curl can be used to estimate whether static nodes exist, and the external curl can be used to determine whether redundant active nodes exist.

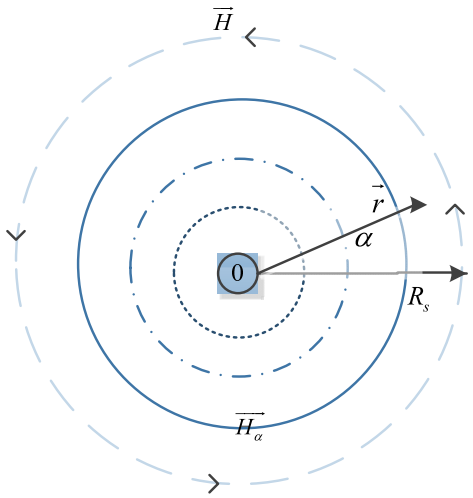

FIGURE 3. The perception model of the node signal.

Consider the perception model of the signal strength that is shown in Fig. 3, where R_s is the radius of the spherical range and I is the strength of the signal vector. Additionally, we assume that the signal strength is evenly distributed over the coverage radius; then, the external curl of the effective communication radius of the active node can be calculated as:

$$rotH_{ex} = (\frac{1}{r}\frac{\partial H_z}{\partial \alpha} - \frac{\partial(\frac{I}{2\pi r})}{\partial z})r + (\frac{\partial H_r}{\partial z} - \frac{\partial H}{\partial r})\alpha + (-\frac{\partial(\frac{I}{2\pi})}{\partial r} + \frac{\partial H_r}{\partial \alpha})k = 0$$

An external curl of zero indicates that the RF signals of static nodes cannot be detected. In this case, the path planning of the active node can be used to establish a multihop communication link and fill in a blank area.

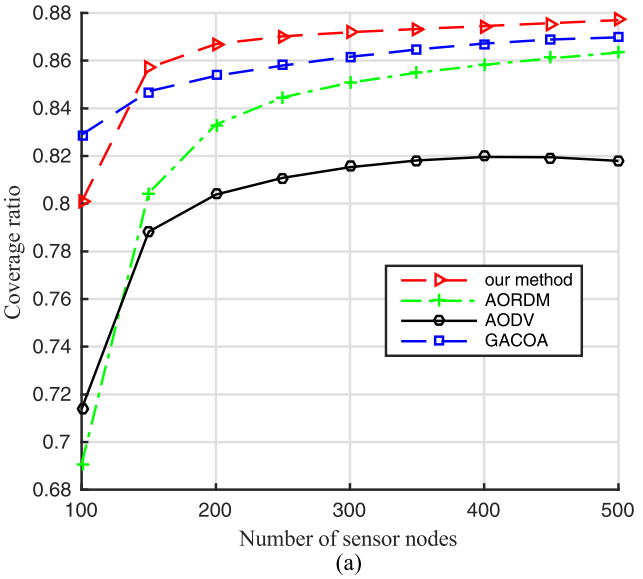

FIGURE 4. The coverage ratio versus the number of nodes and the speed. (a) Impact of the number of nodes on the coverage ratio. (b) Impact of the node movement speed on the coverage ratio.

On the other hand, the internal curl can be computed as:

$$rotH_{in} = (\frac{1}{r}\frac{\partial H_z}{\partial \alpha} - \frac{\partial(\frac{rI}{2\pi R_s^3})}{\partial z})r + (\frac{\partial H_r}{\partial z} - \frac{\partial H_z}{\partial r})\alpha + (\frac{\partial(\frac{rI}{2\pi R_s^3})}{\partial r} - \frac{\partial H_r}{\partial \alpha})\frac{k}{r} = \frac{I}{\pi R_s^2}\vec{k}$$

Obviously, when the internal curl at each point in the effective area covered by the communication radius of the active node is not zero, the signal strength has a constant value of $\frac{I}{\pi R_s^2}$. This indicates that the active node has detected signals coming from nodes at the edge of the blank coverage area. As a consequence, a communication path is established. The active node becomes a relay node and fills in a blank coverage area.

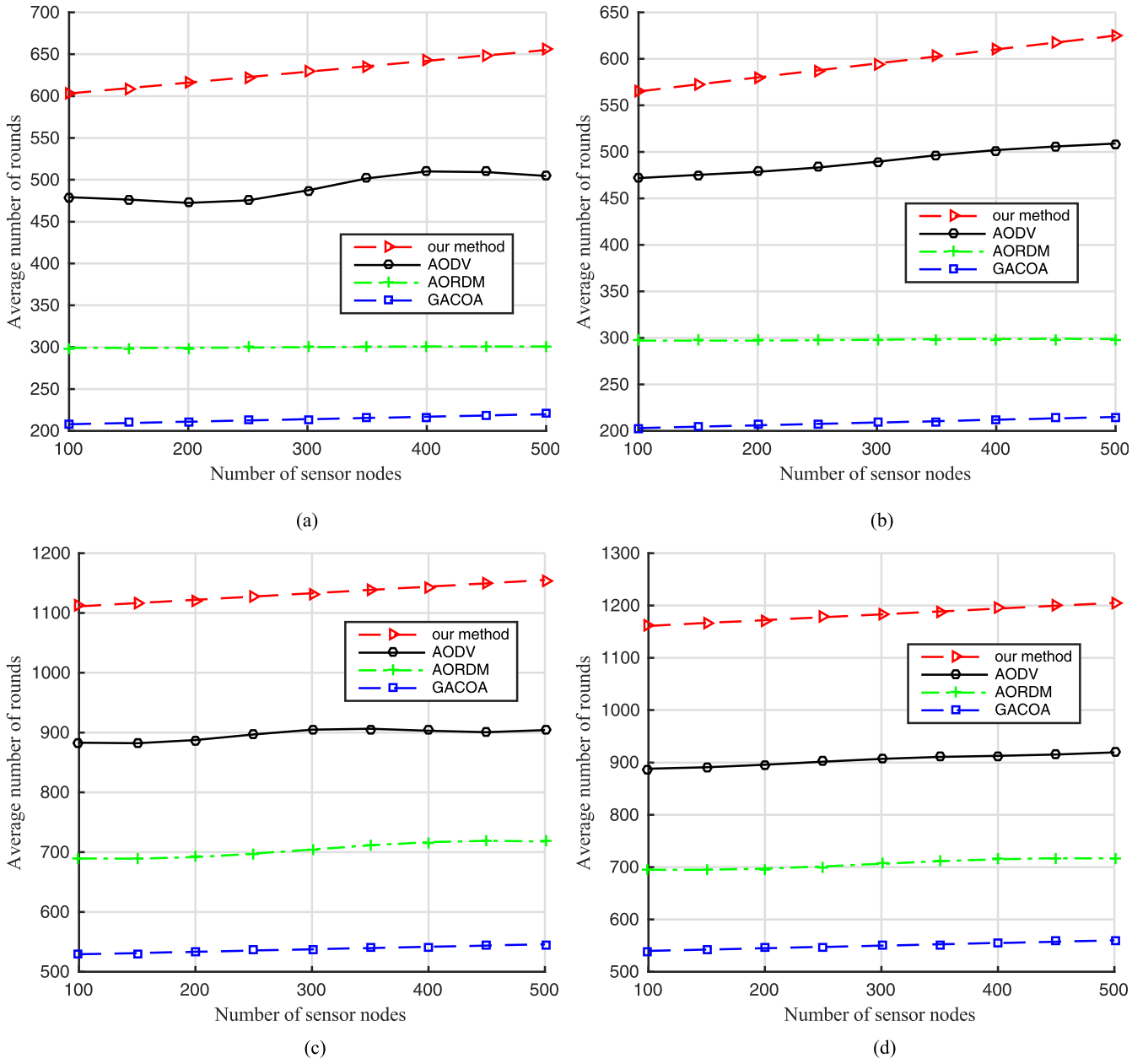

FIGURE 5. Network lifecycle versus the number of sensors. (a) Simulations when the first node dies. (b) Simulations when 25% of the nodes are dead. (c) Simulations when 50% of the nodes are dead. (d) Simulations when 75% of the nodes are dead.

IV. EXPERIMENT

At present, many algorithms for studying network optimal coverage are mostly applied in static networks, and are not suitable for dynamic networks and hybrid networks. Since this paper considers a typical dynamic network environment, many algorithms cannot achieve convincing results in terms of coverage, network life cycle, transmission delay, transmission reliability, load balancing and other indicators. Therefore, the AODV, AORDM and GACOA algorithms are chosen for comparison because they are considered to be effective and advanced in a dynamic network environment. All simulations were conducted on a computer with a 2.1 GHz CPU and 8 GB of RAM.

A. SETTINGS

First, 100–500 nodes were randomly deployed in a rectangular area of 500 m × 500 m. Each active node moved for 20 seconds each time. To account for the randomness of the initial topology of the active nodes, a total of 300 simulations were performed in this experiment. The signal transmission model used in this paper is the spatial transmission loss model [18], [25]. The ideal received signal strength (RSS) of an active node is expressed as:

$$RSS(d) = P_T - 10 \times \eta \times \log_{10}(d) + X_\sigma$$

where P_T is the transmit power of the node, η is the path attenuation factor, d is the distance between the active node and

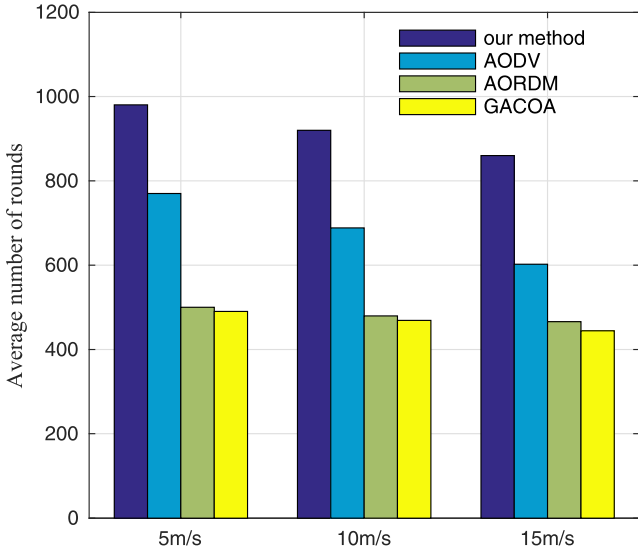

FIGURE 6. Impact of the node movement speed on the network lifecycle.

the target node, and X_σ is the observed noise. Following [13], the parameters were set to $P_T = 55dBm$, $\eta = 4$ (outdoors), mean $X_\sigma = 0$, and variance $\sigma = 5$. In addition, the network delay was set to 3 seconds according to [13], [26], and [27], and the run time was 300 seconds. For consistency with several real applications, e.g., indoor positioning, geological detection and water quality monitoring, the speeds of the mobile nodes were set to 5 m/s, 10 m/s and 15 m/s. Finally, we computed the average values of the simulated results.

B. RESULTS

1) COVERAGE RATIO

Fig. 4(a) shows the relationship between the network coverage and the number of nodes. The coverage increases as the number of sensor nodes increases. When the number of sensor nodes is less than 150, the coverage of the algorithm is greatly affected by the number of nodes; however, when the number of nodes is greater than 150, the coverage increases only slowly with the increase in the number of nodes. Overall, the coverage of our method is higher than those of AODV, AORDM and GACOA when a large number of nodes are deployed, but it is lower than that of GACOA when a small number of nodes are deployed. The reason why this happens is that when the number of nodes is less than 150, the coverage area of the node is significantly smaller than the monitoring area; but when the number of nodes is greater than 150, the overall coverage of the network will be significantly improved even if the node coverage is redundant. This may be related to the specific settings of the network, such as the detection area and the effective communication radius of the Zigbee node.

Fig. 4(b) shows the simulation results for the coverage ratio. The coverage ratio increases as the node speed increases. However, the proposed method has a higher coverage ratio than the other methods at all three speeds (5 m/s, 10 m/s and 15 m/s).

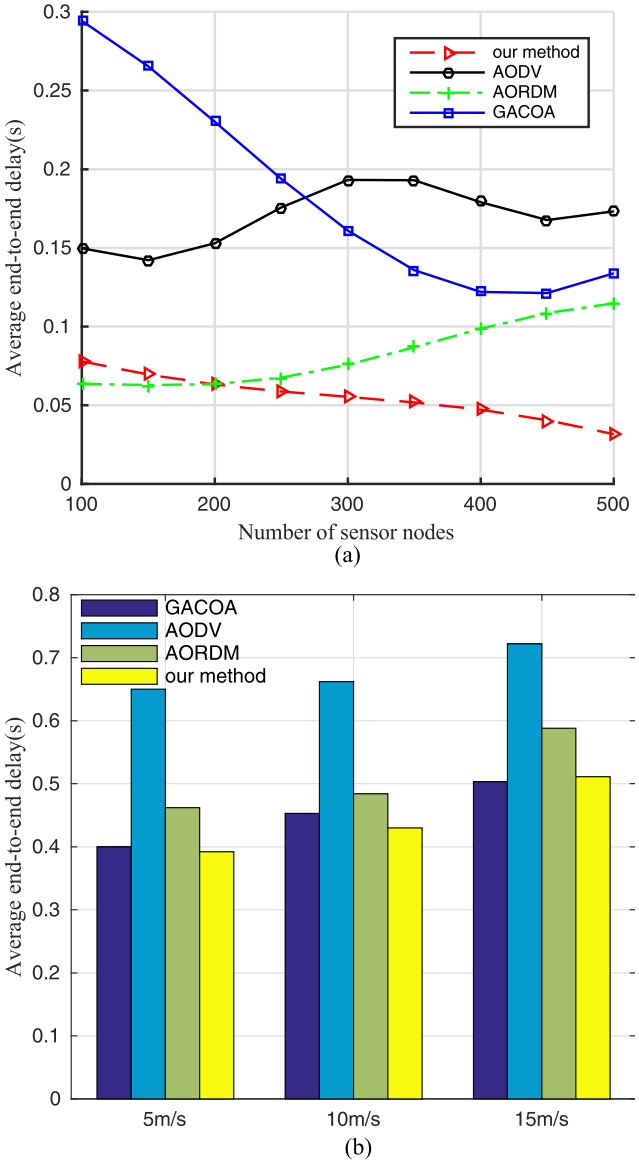

FIGURE 7. The end-to-end delay versus the number of nodes and the speed. (a) Impact of the number of nodes on the end-to-end delay. (b) Impact of the node movement speed on the end-to-end delay.

2) LIFECYCLE

Fig. 5 shows the effect of the node density on the network lifecycle. Fig. 5(a) shows the results for the communication round when the first node dies at different node densities, and Fig. 5(b-d) shows the results for the communication rounds when 25%, 50% and 75% of the nodes are dead. These figures show that AORDM and GACOA have the lowest performance in terms of the network lifecycle, whereas AODV has better residual performance than the traditional routing scheme. The proposed method considers the global optimal coverage and the sum of the remaining energy among the nodes. It selects the appropriate active nodes to establish transmission paths. Therefore, the lifecycle of our method is better than those of the other methods.

Fig. 6 shows the lifecycles at different node speeds. As the node speed increases, the network lifecycle decreases for

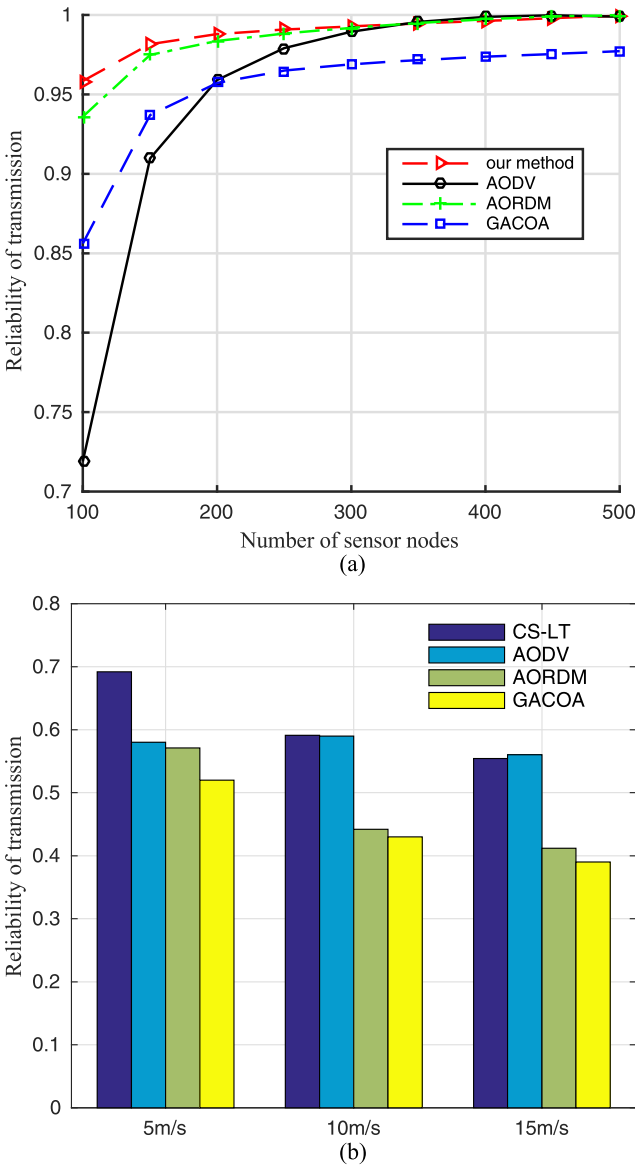

FIGURE 8. The reliability versus the number of nodes and the speed. (a) Impact of the number of nodes on reliability. (b) Impact of the node movement speed on reliability.

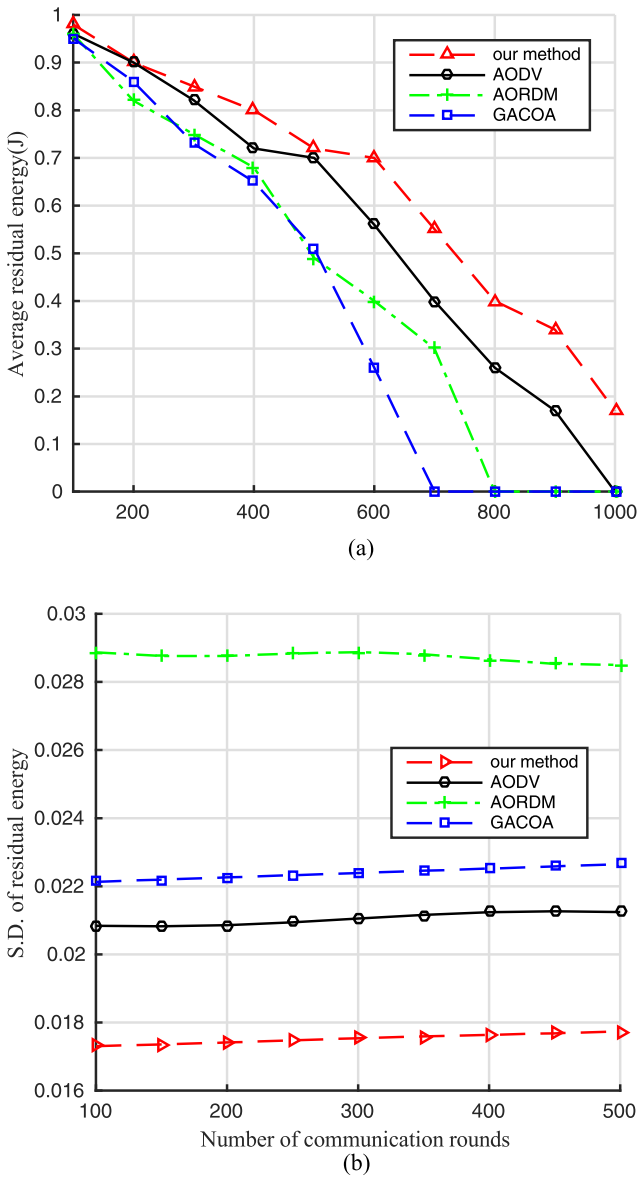

FIGURE 9. The average residual node energy and the standard deviation of the residual node energy versus the number of communication rounds. (a) Impact of the number of communication rounds on the average residual energy. (b) Impact of the number of communication rounds on the standard deviation of the residual energy.

all methods. However, the algorithm proposed in this paper is superior to the other methods.

3) TRANSMISSION DELAY

The average end-to-end delays are shown in Fig. 7(a). The results show that the average delays of GACOA and our method decrease with an increasing number of nodes, whereas the average delays of AODV and AORDM slightly increase as the number of nodes increases. When the network has a low node density, AORDM performs the best in terms of transmission delay. The delay of method is slightly higher than that of AORDM but significantly lower than those of GACOA and AODV. As the node density increases, the delay of our method decreases below that of AORDM; thus, our method becomes the optimal algorithm with respect to the transmission delay.

Fig. 7(b) shows that our algorithm's communication delay is lower than that of AODV and is equivalent to those of AORDM and GACOA at node movement speeds of 5 m/s and 10 m/s.

4) RELIABILITY

Fig. 8(a) shows the effect of the node density on the transmission reliability. This plot shows that the transmission reliability of our method is better than those of AODV and GACOA and is equivalent to that of AORDM. As the number of

sensor nodes increases, the number of transmission paths also increases. The increase in the number of paths is generally caused by probabilistic connections between nodes. When the probability is greater than a certain value, the source node will select the optimal path along which to send the packet to the target node. In each round of communication, some nodes on the transmission path will die. Our method uses active nodes as relays to replace dead nodes, thereby ensuring reliable transmission and avoiding information loss.

Fig. 8(b) compares the transmission reliabilities at different node movement speeds. The performance of our method is slightly better than that of AODV at a speed of 5 m/s. However, our method is comparable to AODV at higher speeds, i.e., 10 m/s and 15 m/s. In all cases, AORDM and GACOA have lower transmission reliability.

5) LOAD BALANCE

Fig. 9(a) and Fig. 9(b) show the load balance after communication, which is measured in terms of the average residual energy among the nodes and the standard deviation of the node energies. As seen in Fig. 9(a), as the number of communication rounds increases, the proposed algorithm achieves the highest average residual energy. The energy consumption curve of our method is also smoother than those of the other methods. This indicates that the movement paths of the active nodes can be effectively planned. Fig. 9(b) shows that the standard deviation of the residual node energies with the proposed algorithm is also the smallest at the end of each 50 rounds of communication. This is because active nodes replace dead nodes and fill in blank areas through path planning, helping the sensor nodes on the communication paths to consume energy more evenly.

V. CONCLUSION

This paper proposes an active node communication strategy for optimal coverage, which provides a feasible solution to the problems posed by limited communication radii and a dynamic network topology. The method uses active nodes to transfer data to static nodes and replace failed nodes. The results show that without stringent location requirements, the proposed method can improve communication performance in terms of the network coverage and lifecycle, transmission delay, transmission reliability and load balance. This method can be applied in sensor networks intended for various applications, such as indoor positioning, mountain monitoring and water pollution tracking. In the future, we will expand this work to improve the transmission reliability and energy efficiency in more complex environments, such as wireless mesh networks and ad hoc networks.

ACKNOWLEDGMENT

(Tao Xie and Chunjiong Zhang contributed equally to this work.) The authors declare that they have no competing interests.

REFERENCES

[1] X. Jia, L. Yang, and H. Zhu, "Cognitive opportunistic relaying systems with mobile nodes: Average outage rates and outage durations," *IET Commun.*, vol. 8, no. 6, pp. 789–799, Apr. 2014.

[2] B. Xu, Y. Zhu, D. Kim, D. Li, H. Jiang, and A. O. Tokuta, "Strengthening barrier-coverage of static sensor network with mobile sensor nodes," *Wireless Netw.*, vol. 22, no. 1, pp. 1–10, 2016.

[3] F. G. H. Yap and H.-H. Yen, "A survey on sensor coverage and visual data capturing/processing/transmission in wireless visual sensor networks," *Sensors*, vol. 14, no. 2, pp. 3506–3527, 2014.

[4] N. Hu, C. Wu, P. Liu, H. Wu, B. Wu, and L. Cheng, "Vote selection mechanisms and probabilistic data association-based mobile node localization algorithm in mixed LOS/NLOS environments," *Telecommun. Syst.*, vol. 62, pp. 641–655, Aug. 2016.

[5] S. Mottaghi and M. R. Zahabi, "Optimizing LEACH clustering algorithm with mobile sink and rendezvous nodes," *AEU-Int. J. Electron. Commun.*, vol. 69, pp. 507–514, Feb. 2015.

[6] S. K. Singh, P. Kumar, and J. P. Singh, "A survey on successors of LEACH protocol," *IEEE Access*, vol. 5, pp. 4298–4328, 2017.

[7] A. Sayyed, G. M. de Araújo, J. P. Bodanese, and L. B. Becker, "Dual-stack single-radio communication architecture for UAV acting as a mobile node to collect data in WSNs," *Sensors*, vol. 15, no. 9, pp. 23376–23401, 2015.

[8] J. Zhao, H. Li, and X. Sun, "Research on the signal random attenuation coefficient based on RSSI in WSN localization technology," in *Proc. 5th Int. Conf. Wireless Commun., Netw. Mobile Comput. (WiCom)*, Sep. 2009, pp. 1–4.

[9] Y. Zhong and L. Zhang, "An adaptive artificial immune network for supervised classification of multi-/hyperspectral remote sensing imagery," *IEEE Trans. Geosci. Remote Sens.*, vol. 50, no. 3, pp. 894–909, Mar. 2012.

[10] Y. Li, Z. Wang, L. Su, D. Jin, and S. Chen, "An optimal relaying scheme for delay-tolerant networks with heterogeneous mobile nodes," *IEEE Trans. Veh. Technol.*, vol. 62, no. 5, pp. 2239–2252, Jun. 2013.

[11] Y. Yao, J. Liu, and N. N. Xiong, "Privacy-preserving data aggregation in two-tiered wireless sensor networks with mobile nodes," *Sensors*, vol. 14, no. 11, pp. 21174–21194, 2014.

[12] X. M. Zhang, Y. Zhang, F. Yan, and A. V. Vasilakos, "Interference-based topology control algorithm for delay-constrained mobile ad hoc networks," *IEEE Trans. Mobile Comput.*, vol. 14, no. 4, pp. 742–754, Apr. 2015.

[13] P. Dini, J. N. Guerrero, and N. Baldo, "An overlay and distributed approach to node mobility in multi-access wireless networks," *Wireless Netw.*, vol. 20, no. 6, pp. 1275–1293, 2014.

[14] Z. M. Fadlullah, D. Takaishi, H. Nishiyama, N. Kato, and R. Miura, "A dynamic trajectory control algorithm for improving the communication throughput and delay in UAV-aided networks," *IEEE Netw.*, vol. 30, no. 1, pp. 100–105, Jan./Feb. 2016.

[15] Z. Taifei, G. Yingying, and Z. Ying, "An area coverage algorithm for non-line-of-sight ultraviolet communication network," *Photonic Netw. Commun.*, vol. 32, pp. 269–280, Oct. 2016.

[16] J. F. Colom, H. Mora, D. Gil, and M. T. Signes-Pont, "Collaborative building of behavioural models based on Internet of Things," *Comput. Elect. Eng.*, vol. 58, pp. 385–396, Feb. 2017.

[17] M. Mozaffari, W. Saad, M. Bennis, and M. Debbah, "Efficient deployment of multiple unmanned aerial vehicles for optimal wireless coverage," *IEEE Commun. Lett.*, vol. 20, no. 8, pp. 1647–1650, Aug. 2016.

[18] J. Zhu and B. Wang, "The optimal placement pattern for confident information coverage in wireless sensor networks," *IEEE Trans. Mobile Comput.*, vol. 15, no. 4, pp. 1022–1032, Apr. 2016.

[19] M. Ahmadi, M. Shojafar, A. Khademzadeh, K. Badie, and R. Tavoli, "A hybrid algorithm for preserving energy and delay routing in mobile ad-hoc networks," *Wireless Pers. Commun.*, vol. 85, no. 4, pp. 2485–2505, 2015.

[20] C. Gao, Y. Li, Y. Zhao, and S. Chen, "A two-level game theory approach for joint relay selection and resource allocation in network coding assisted D2D communications," *IEEE Trans. Mobile Comput.*, vol. 16, no. 10, pp. 2697–2711, Oct. 2017.

[21] K. Jeddisaravi, R. J. Alitappeh, L. C. A. Pimenta, and F. G. Guimarães, "Multi-objective approach for robot motion planning in search tasks," *Appl. Intell.*, vol. 45, pp. 305–321, Sep. 2016.
[22] M. Fathian and A. R. Jafarian-Moghaddam, "New clustering algorithms for vehicular ad-hoc network in a highway communication environment," *Wireless Netw.*, vol. 21, no. 8, pp. 2765–2780, 2015.
[23] Z. Yang, J. Dou, J. Du, and Z. Gao, "Large radius of curvature measurement based on the evaluation of interferogram-quality metric in non-null interferometry," *Opt. Commun.*, vol. 410, pp. 756–762, Mar. 2018.
[24] K. Watanabe, "Elastodynamic Doppler effects and wave energy partition by a sliding interface," *Acta Mechanica*, vol. 228, no. 12, pp. 4169–4186, 2017.
[25] M. Hammoudeh and R. Newman, "Adaptive routing in wireless sensor networks: QoS optimisation for enhanced application performance," *Inf. Fusion*, vol. 22, no. 1, pp. 3–15, Mar. 2015.
[26] E. M. Royer and C. E. Perkins, "Ad-hoc on-demand distance vector routing," in *Proc. 2nd IEEE Workshop Mobile Comput. Syst. Appl.*, Feb. 1999, pp. 90–100.
[27] J. D. Phillips and D. Stanovský, "Automated theorem proving in quasigroup and loop theory," *Ai Commun.*, vol. 23, pp. 267–283, Jan. 2010.

Authors' photographs and biographies not available at the time of publication.